BBA - Molecular Cell Research 1873 (2026) 120101

Contents lists available at ScienceDirect

BBA - Molecular Cell Research

journal homepage: www.elsevier.com/locate/bbamcr

Research Paper

# The tumor suppressor role of mitochondrial E3 ubiquitin ligase MUL1 in osteosarcoma

Jacopo Di Gregorio [a], Sara Terreri [b], Michela Rossi [c], Giulia Battafarano [b], Laura Di Giuseppe [b], Olivia Pagliarosi [b,c], Lucia Cilenti [d], Enrico Ricevuto [a], Antonis S. Zervos [d], Vincenzo Flati [a,*,1], Andrea Del Fattore [b,1]

[a] Department of Biotechnological and Applied Clinical Sciences, University of L'Aquila, L'Aquila, Italy
[b] Bone Physiopathology Research Unit, Translational Pediatric and Clinical Genetic Research Division, Bambino Gesù Children's Hospital, IRCCS, Rome, Italy
[c] Department of Medical and Cardiovascular Sciences, Sapienza University, Rome, Italy
[d] Burnett School of Biomedical Sciences, University of Central Florida, College of Medicine, Orlando, FL, USA

ARTICLE INFO

*Keywords:*
Osteosarcoma
Cancer Metabolism
MUL1
HIF-1α

ABSTRACT

Osteosarcoma is a highly aggressive type of bone cancer with a high rate of metastasis. The molecular mechanisms underlying osteosarcoma metastasis are not yet completely understood, representing an ongoing challenge for therapy. A possible therapeutic target is the hypoxia-inducible factor HIF-1α which is upregulated in metastatic osteosarcoma. Indeed, HIF-1α promotes proliferation, resistance to apoptosis and metabolic reprogramming towards glycolysis, whereas its downregulation increases apoptosis. The molecular mechanism mediated by the mitochondrial E3 ubiquitin ligase MUL1 could be exploited to target HIF-1α since low MUL1 protein levels result in HIF-1α accumulation and activity even under normoxic conditions, while high levels of MUL1 promote HIF-1α degradation. Here, we show that MUL1 protein levels inversely correlate with the aggressiveness of osteosarcoma cell lines. Induction of MUL1 in aggressive cells reduces HIF-1α levels, paired with a decrease in proliferation, migration and glycolysis and increase in apoptosis, whereas MUL1 inactivation in low-aggressive cells has opposite results. Therefore, the modulation of MUL1 protein levels affects cell proliferation, migration, apoptosis, and metabolism. This is the first report that reveals a tumor suppressor role for MUL1 in osteosarcoma, and suggests MUL1 induction as a potential therapeutic strategy to reduce HIF-1α activity in the metastatic progression of this cancer.

## 1. Introduction

Osteosarcoma is a highly aggressive bone tumor that frequently occurs in pediatric patients [1]. Although relatively rare, it represents the most common primary bone cancer and predominantly targets skeletal sites with high turnover, such as the distal femur and proximal tibia. Metastasis, particularly to the lung, is a frequent complication in osteosarcoma patients [2]. Currently, therapeutic strategies rely on surgical resection combined with neoadjuvant or adjuvant chemotherapy [3]. Although in non-metastatic disease these approaches have improved patient survival rates by approximately 65 %, patients diagnosed with metastases still face the poorest prognosis, with 5-year survival rates of around 19 % [4]. In addition, chemoresistance remains an unresolved complication, which often requires a higher drug dosage that can cause severe side-effects [4].

For these reasons, the identification of novel targets is necessary to develop new therapeutic approaches for osteosarcoma. Unfortunately, the mechanisms and signaling pathways driving osteosarcoma progression, and most importantly metastasis, have not been fully elucidated yet [5]. Several potential mechanisms of metastasis in osteosarcoma have been identified, including genomic instability [6] or the activation of the PI3K/AKT/mTOR [7] and Transforming Growth Factor-β (TGF-β) signaling pathways [8]. These pathways are known to promote epithelial-to-mesenchymal transition (EMT), a process of

* Corresponding author at: Department of Biotechnological and Applied Clinical Sciences, University of L'Aquila, 67100, L'Aquila, Italy.
*E-mail addresses:* jacopo.digregorio@guest.univaq.it (J. Di Gregorio), sara.terreri@opbg.net (S. Terreri), michela1.rossi@opbg.net (M. Rossi), giulia.battafarano@opbg.net (G. Battafarano), laura.digiuseppe@opbg.net (L. Di Giuseppe), olivia.pagliarosi@opbg.net (O. Pagliarosi), cilenti774@gmail.com (L. Cilenti), enrico.ricevuto@univaq.it (E. Ricevuto), Antonis.Zervos@ucf.edu (A.S. Zervos), vincenzo.flati@univaq.it (V. Flati), andrea.delfattore@opbg.net (A. Del Fattore).
[1] These authors contributed equally to this work.

https://doi.org/10.1016/j.bbamcr.2025.120101
Received 19 August 2025; Received in revised form 22 December 2025; Accepted 24 December 2025
Available online 28 December 2025

cellular plasticity in which epithelial cells acquire mesenchymal features, leading to enhanced motility and invasiveness [9].

Moreover, great interest has been attracted by the study of cancer metabolic reprogramming, whereby tumor cells rewire their metabolism, most notably by upregulating aerobic glycolysis to sustain the increased energy demands. Depending on cancer type, several metabolic pathways may be altered, leading to increased tumor proliferation. In osteosarcoma, several metabolism-related genes are dysregulated; in the context of metastasis, osteosarcoma cells preferentially switch to aerobic glycolysis [10]. This process is largely mediated by hypoxia-inducible factor HIF-1α, a transcription factor that normally regulates cell adaptation to hypoxia [11]. Under normoxia, HIF-1α is rapidly degraded; under hypoxia, HIF-1α translocates to the nucleus and stimulates the expression of more than 100 genes containing the Hypoxia-Responsive Element (HRE) in the promoter or enhancer regions [11]. These genes regulate cell survival, proliferation, angiogenesis, and aerobic glycolysis at the expense of oxidative phosphorylation (OXPHOS) [11]. Cancer cells could increase their proliferation rate and survival by HIF-1α hyperactivation through alterations of the Cullin Ring Ligase 2/Von Hippel Lindau ($CRL2^{VHL}$) complex, which is normally responsible for HIF-1α ubiquitination and degradation by the proteasome [12]. In osteosarcoma, HIF-1α is upregulated and its expression positively correlates with metastatic potential, making it a marker of poor prognosis [13]. *In vitro* experiments have demonstrated that HIF-1α silencing by siRNA reduces proliferation and induces apoptosis in osteosarcoma cells, highlighting its potential as a therapeutic target [14].

Our previous studies have identified a novel pathway, mediated by the activity of the mitochondrial E3 ubiquitin ligase MUL1, that regulates the protein levels of HIF-1α. MUL1 (also known as Mulan, MAPL, GIDE, and HADES) is one of three mitochondrial E3 ligases. Although located in the outer mitochondrial membrane, its catalytic RING domain faces the cytoplasm [15], enabling MUL1 to act as an E3 ubiquitin or a Small Ubiquitin-Like Modification (SUMO) ligase on cytosolic targets. By mediating K-63 or K-48 linked ubiquitination, as well as SUMOylation, of several substrates, MUL1 has been implicated in apoptosis, mitophagy, innate immune response, and, as we have recently demonstrated, cellular metabolism [16–20].

MUL1 indirectly regulates HIF-1α *via* K-48 linked ubiquitination and degradation of UBX Domain Protein 7 (UBXN7), a scaffold protein and cofactor of the $CRL2^{VHL}$ complex [17]. The complex is responsible for the ubiquitination of HIF-1α, followed by its degradation through the proteasome. Controlled UBXN7 levels are essential for proper $CRL2^{VHL}$ assembly and efficient HIF-1α degradation [17]. Inactivation of MUL1, by mutation or by excessive activity of the mitochondrial serine protease High Temperature Requirement Serine Peptidase 2 (HTRA2) [21], leads to UBXN7 accumulation, impaired $CRL2^{VHL}$ activity and functional increase of HIF-1α, even under normoxia. This, in turn, drives a metabolic switch towards glycolysis. Conversely, high MUL1 activity promotes UBXN7 degradation, resulting in HIF-1α downregulation and a metabolic phenotype mainly reliant on OXPHOS [18].

The MUL1-UBXN7-HIF-1α axis could be relevant in cancer, where MUL1 is known to play a context-dependent role as either an oncogene or a tumor suppressor, depending on its substrates and cancer type [22]. However, the function of MUL1 in osteosarcoma has never been investigated, despite evidence implicating dysregulation of ubiquitination in this tumor [23].

Here, we provide the first evidence supporting a tumor suppressor role for MUL1 in osteosarcoma. We show that the MUL1-UBXN7-HIF-1α pathway is dysregulated in osteosarcoma cell lines with different degrees of aggressiveness, and that MUL1 modulation affects HIF-1α protein levels, proliferation, migration, apoptosis, and glycolytic activities. Based on these findings, we propose that restoring MUL1 expression in osteosarcoma could represent a promising strategy for novel therapies for this cancer.

## 2. Materials and methods

### 2.1. Patients data and survival curves

Osteosarcoma patient datasets and survival rates were obtained using the software "R2: Genomics Analysis and Visualization Platform" (http://r2.amc.nl http://r2platform.com). Kaplan-Meier curves were generated with the same software. A dataset consisting of genome-wide gene expression profiles from high-grade osteosarcoma samples [24] was used for the analyses. Overall and Metastasis-free survival were analyzed in patients with a known anatomical site of the primary tumor (axial, femur, humerus, ilium, pelvis, tibia/fibula). Patients were then stratified according to MUL1/HTRA2 expression.

### 2.2. Cell culture and chemicals

Human osteosarcoma cell lines Saos-2 (RRID:CVCL_0548), HOS (RRID:CVCL_0312), and 143B (RRID:CVCL_2270) were purchased from American Type Culture Collection (ATCC, VA, USA), and cultured in Dulbecco's Modified Eagle's Medium (DMEM) supplemented with 10 % Fetal Bovine Serum (FBS), 2 mM L-glutamine, 50 μg/ml streptomycin, 50 U/ml penicillin (all from Euroclone, Milano, Italy). Cells were maintained at 37 °C in a humidified atmosphere containing 5 % $CO_2$. For treatments, $3 \times 10^5$ cells were plated and treated with either 20 μM Ucf-101 (provided by the University of Central Florida) for 48 h, 50 nM Chetomin for 24 h, 20 nM Echinomycin for 24 h, 2 μM Cisplatin for 24 h, 100 nM Methotrexate for 5 days (all from ChemCruz, SantaCruz Biotechnology, TX, USA), 100 μM Cobalt Chloride for 6 h (Sigma-Merck, Milano, Italy), 25 or 50 nM Carfilzomib for 4 h (Thermo Fisher Scientific, MA, USA), 20 μM PX-478 for 24 h (SelleckChem, Cologne, NA). Control cells were treated with an equal volume of DMSO (Sigma-Aldrich, MO, USA) as vehicle (Veh). All experiments were carried out using mycoplasma-free cells.

### 2.3. Expression vectors and siRNA transfection

For overexpression experiments, $3 \times 10^5$ osteosarcoma cells/well were seeded in 6-well plates and cultured for 24 h; cells were then transfected with 1 μg of pEGFP (empty vector), pMUL1 (to overexpress MUL1), or pMUL1 C/A (encoding a catalytically inactive MUL1 mutant lacking E3 ligase activity, generated by replacing cysteine 339 with alanine) using Lipofectamine 3000 reagent (Thermo Fisher Scientific, MA, USA), according to the manufacturer's instructions. Each construct contained a green fluorescent protein (GFP) tag and was generated as previously described [17]. For siRNA experiments, cells were transfected with 50 nM of negative control siRNA (Silencer™ Negative Control No. 1) or siRNA against HIF1A (both from Thermo Fisher Scientific, MA, USA) using Lipofectamine RNAiMAX (Thermo Fisher Scientific, MA, USA). After 48 h, protein expression was evaluated by Western Blot analysis.

### 2.4. Generation of Saos-2 MUL1 −/− cell line using CRISPR/Cas9

To generate a MUL1 KO (knock-out) cell line, a MUL1-specific target sequence (5′–GCCGCCGTCATGGAGAGCGG–3′), located in exon 1, was cloned into the pSpCas9(BB)-2A-Puro vector (Addgene plasmid PX459), as previously described [20]. The resulting construct (PX459-Mul1-target) and the empty PX459 control vector were transfected into Saos-2 cells; transfected cells were selected by puromycin treatment, and single clones were expanded. MUL1 protein expression was monitored by Western Blot analysis. Two independent KO clones (Saos-2 MUL1 −/−) and control clones (Saos-2 MUL1 +/+) were selected for the subsequent experiments.

### 2.5. SDS-PAGE and Western Blot analysis

Cells were lysed using radioimmunoprecipitation assay buffer (RIPA, Sigma-Aldrich, MO, USA) supplemented with a protease inhibitor mix (Protease Inhibitor Cocktail, Sigma-Aldrich, MO, USA) and incubated for 30 min on ice. Forty μg of the protein lysates were resolved by SDS-Polyacrylamide gel electrophoresis (PAGE), transferred into PVDF membranes (Biorad, CA, USA), and placed in 4 % nonfat dry milk in TBST buffer (25 mM Tris-HCl pH 8.0, 125 mM NaCl, 0.1 % Tween 20) to block nonspecific binding of the membrane. The membranes were then incubated with the indicated primary antibodies: MUL1, UBXN7, and HTRA2 (rabbit polyclonal antibodies, homegrown, 1:5000) [17], HIF-1α (Bioss Antibodies, 1:2000), β-Actin (SantaCruz, 1:2000), PARP/Cleaved PARP (Cell Signaling, 1:1000), and Caspase 3/Cleaved Caspase 3 (Cell Signaling, 1:1000). Secondary peroxidase-conjugated goat anti-rabbit or goat anti-mouse antibodies (BioRad Laboratories, CA, USA) were used at 1:5000 dilution. Protein bands were detected by enhanced chemiluminescence (ECL) (BioRad Laboratories, CA, USA) using the Image-Quant LAS 4000 biomolecular imager. Densitometric analysis was performed using the ImageJ software (ImageJ, U. S. National Institutes of Health, MD, USA, https://imagej.net/ij/).

### 2.6. Apoptosis assay

After transfection and drug treatment, cells were resuspended in Binding Buffer, stained with Annexin V and propidium iodide using the *Tali* apoptosis kit (Thermo Fisher Scientific, Milano, Italy), and analyzed using the *Tali*-image assisted cytometer (Thermo Fisher Scientific, Milano, Italy) according to the manufacturer's instructions [25].

### 2.7. Proliferation assay

Cell proliferation was assessed using the CCK8-Cell Counting Kit (Dojindo Lab, Munich, Germany), following the manufacturer's instructions. After incubation at 37 °C for 2 h, Optical Density (O.D.) was measured at 450 nm using a microplate reader (BMG Labtech, Ortenberg, Germany).

### 2.8. Migration assay

143B and Saos-2 cells were cultured in 12-well plates until full confluence was reached. Then, a scratch was made at time 0. Detached cells and cellular debris were removed by washing with PBS (Phosphate Buffered Solution); images were captured at time 0 and after 8 h for 143B, at time 0 and after 24 h for Saos-2 cells. The distance between the two wound edges was measured by ImageJ software. Wound closure was calculated as the difference between the wound width at time 0 and at the end of the experiments.

### 2.9. Metabolic analyses

All metabolic analyses were performed using the SeaHorse XFe96 Extracellular Flux Analyzer (Agilent Technologies, Milano, Italy). Cells were seeded in quintuplicate at a density of 10.000 per well and cultured for 24 h. Medium was then exchanged with assay medium (XF DMEM medium pH 7.4 supplemented with 10 mM glucose, 2 mM glutamine, 1 mM pyruvate, all from Agilent Technologies, Milano, Italy), followed by incubation at 37 °C in a non-$CO_2$ incubator for 60 min. Then Oxygen Consumption Rate (OCR) and Extracellular Acidification Rate (ECAR) were measured. For Glycolysis measurement, the Seahorse XF Glycolytic Rate Assay kit was used (Agilent Technologies, Milano, Italy). ECAR was measured in basal conditions and after sequential injections of mitochondrial electron transport chain inhibitors Rotenone/Antimycin (5 μM) and glycolysis inhibitor 2-deoxyglucose (2-DG) (300 mM). Basal glycolysis was evaluated as ECAR before the addition of inhibitors, whereas compensatory glycolysis was measured as ECAR after the addition of mitochondrial inhibitors. To analyze ATP production, the XF Real Time ATP Rate Assay was used. ECAR and OCR were measured under basal conditions, and after the injections of 1.5 μM oligomycin and 0.5 μM rotenone/antimycin. Finally, to assess mitochondrial stress, the SeaHorse XF MitoStress Test was performed (Agilent Technologies, Milano, Italy). Oxygen consumption rate (OCR) was measured under basal conditions and before the injection of the following compounds: 1.5 μM of oligomycin, 1.0 μM of FCCP, and 0.5 μM rotenone/antimycin. All kits and tests were used following the manufacturer's instructions. Data analysis was performed using the specific Report Generator software (Agilent Technologies, Milano, Italy).

### 2.10. Statistics

All data were expressed as mean ± SD of at least three independent experiments. Values were compared by Student's *t*-test with Welch's correction. For multiple comparisons, values were compared by one-way ANOVA, followed by Tukey's multiple comparison test. A $p$ value $\leq 0.05$ was considered statistically significant. Analyses were performed through GraphPad Prism 10.2.

## 3. Results

### 3.1. Low levels of MUL1 are associated with decreased survival in osteosarcoma

To investigate the role of MUL1 in osteosarcoma, we analyzed osteosarcoma patient datasets and assessed MUL1 expression. Kaplan-Meier analysis showed that patients with higher MUL1 expression had better overall survival probability (Fig. 1A) as well as improved metastasis-free survival (Fig. 1B). Conversely, high expression of HTRA2, the upstream negative regulator of MUL1, was correlated with reduced overall and metastasis-free survival rate (Fig. 1C–D). Additionally, HTRA2 was expressed at an overall higher level compared to MUL1 across the dataset (Fig. 1E), suggesting a further negative regulation of MUL1. Together, these findings suggest that MUL1 may act as a tumor suppressor in osteosarcoma.

### 3.2. MUL1 protein levels inversely correlate with tumor aggressiveness in osteosarcoma cell lines

Since the reduction of MUL1 could be responsible for the increased levels of HIF-1α observed in metastatic osteosarcoma, we evaluated the MUL1-UBXN7-HIF-1α pathway in osteosarcoma cell lines with different aggressiveness: low aggressive Saos-2, more aggressive HOS and highly aggressive and metastatic 143B cells [26]. We observed that MUL1 was expressed in Saos-2, while its protein levels were reduced in HOS and 143B cells (Fig. 2A–B). This protein modulation could depend on post-transcriptional regulation and/or post-translational modification, as it was not due to a decrease of mRNA expression in HOS and 143B cells, which instead showed the opposite trend (Fig. S1). According to the MUL1 protein expression, UBXN7 and HIF-1α protein levels were higher in HOS and 143B when compared to Saos-2 cells (Fig. 2A–B). HTRA2 expression had a trend of increase in 143B cells, suggesting enhanced protease activity. These data indicate that the downregulation of MUL1 protein in aggressive osteosarcoma cells contributes to increased HIF-1α levels through modulation of the MUL1-UBXN7-HIF-1α pathway; indeed, as we previously reported [17,18] and shown in Fig. S2, MUL1 is not able to bind HIF-1α. For the following experiments, we therefore used the 143B and Saos-2 cells, which express the lowest and the highest protein levels of MUL1, respectively.

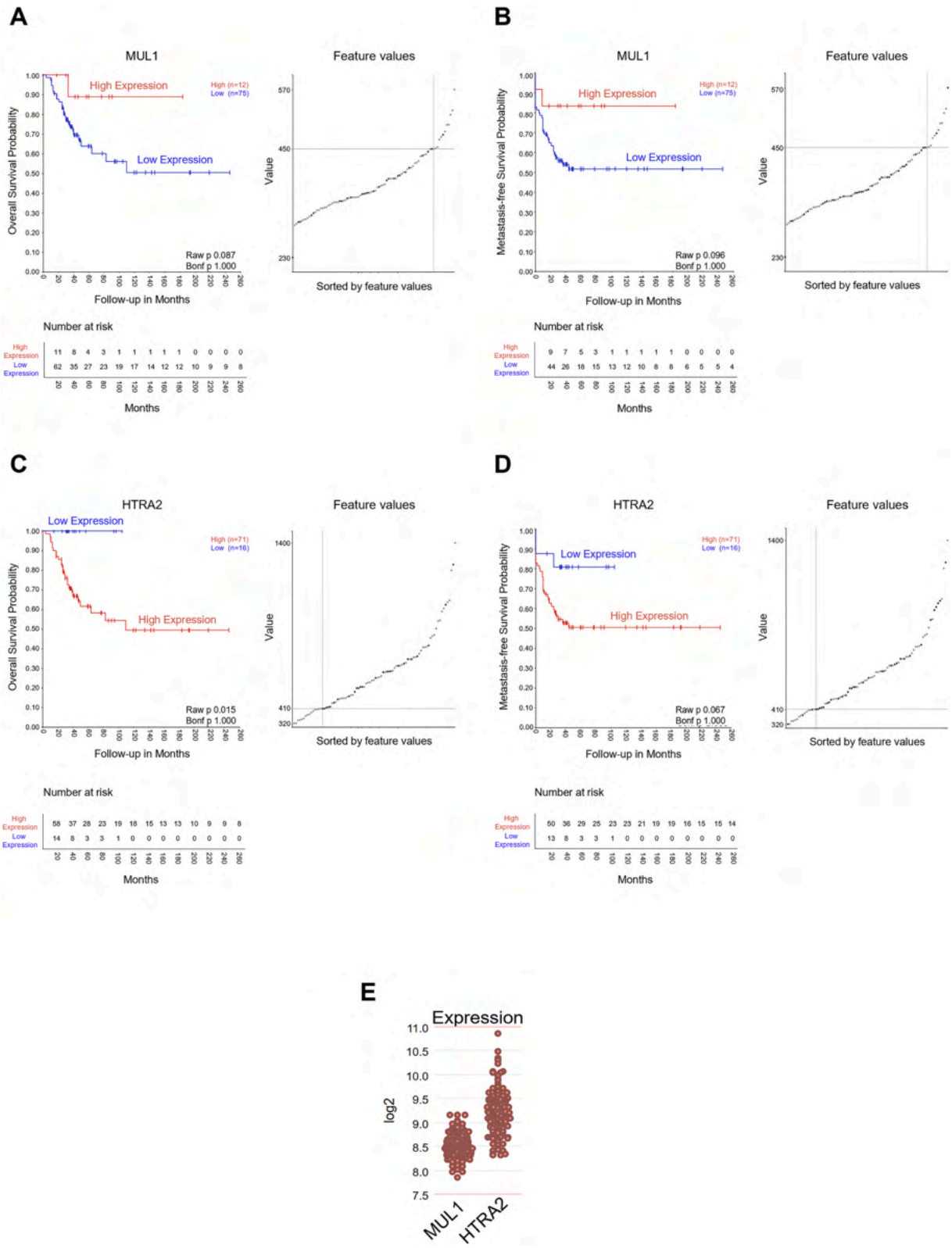


**Fig. 1.** MUL1 and HTRA2 in osteosarcoma patients. A–B) Kaplan-Meier curves, performed on a dataset of 87 osteosarcoma patients, highlighting A) the overall survival and B) metastasis-free survival probability of patients in conditions of high (red) and low (blue) expression of MUL1. The expression graph shows the cut-off values for high and low expression. The number of patients at risk at each time point was also reported according to MUL1 expression. C–D) Kaplan-Meier curves, performed on a dataset of 87 osteosarcoma patients, highlighting C) the overall survival and D) metastasis-free survival probability of patients in conditions of high (red) and low (blue) expression of HTRA2. The expression graph shows the cut-off values for high and low expression. The number of patients at risk at each time point was also reported according to HTRA2 expression. E) Overall expression of MUL1 and HTRA2 in the sample dataset. (For interpretation of the references to color in this figure legend, the reader is referred to the web version of this article.)

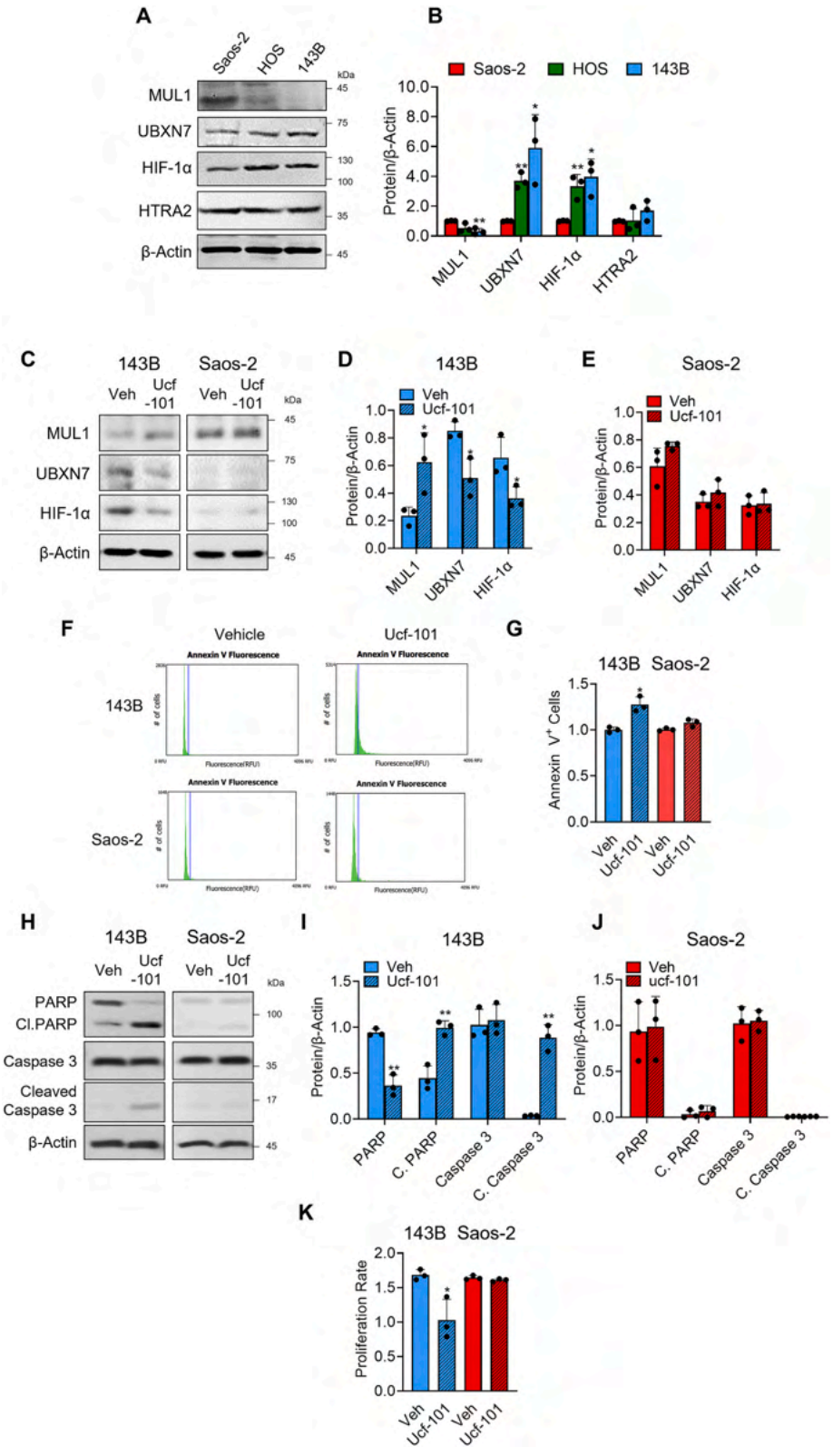


(caption on next page)

**Fig. 2.** Expression of MUL1/HIF-1α pathway in osteosarcoma cell lines and effects of HTRA2 inhibitor Ucf-101. A) Western blot analysis showing the protein levels of MUL1, UBXN7, HIF-1α and HTRA2 in Saos-2 (non-aggressive cells), HOS (aggressive, non-metastatic) and 143B (highly aggressive, highly metastatic) osteosarcoma cell lines. B) Densitometric analysis of the protein bands normalized against β-Actin and compared to Saos-2 cells. Results are expressed as means ± S.D. of three independent experiments.*$p < 0.05$ and **$p < 0.01$ *vs* Saos-2. C) Effects of Ucf-101 on osteosarcoma cell lines. 143B and Saos-2 cell lines were treated with Ucf-101 (20 μM) or DMSO as Vehicle (Veh) for 48 h. Western Blot analysis showing the protein levels of MUL1, UBXN7 and HIF-1α in 143B and Saos-2 cell lines. D–E) Densitometric analysis of the protein bands of D) 143B cells and E) of Saos-2 cells normalized against β-Actin. F) Representative pictures of Annexin V staining, obtained by Tali Apoptosis Kit. G) Quantification of Annexin V+ cells. H) Western Blot analysis showing the protein levels of PARP and Caspase 3, as well as their cleaved forms. I–J) Densitometric analysis of the protein levels from (H) of I) 143B cells and J) Saos-2 cells, normalized against β-Actin. K) Cellular proliferation rate evaluated by CCK8 Cell Counting Kit. In D–E, G, I–K) results are presented as mean ± S.D. of three independent experiments. *$p < 0.05$ and **$p < 0.01$ *vs* respective cells treated with vehicle (Veh).

### *3.3. MUL1 induction by HTRA2 inhibition downregulates UBXN7 and HIF-1α, increasing apoptosis and reducing proliferation in aggressive osteosarcoma cells*

To evaluate how MUL1 modulation influences HIF-1α and tumor features, we treated 143B and Saos-2 cells with the selective HTRA2 inhibitor Ucf-101 [27]. In 143B cells, Ucf-101 treatment significantly increased MUL1 protein levels and concomitantly reduced UBXN7 and HIF-1α expression (Fig. 2C–D). This modulation of the components of the MUL1-HIF-1α pathway by Ucf-101 in 143B cells was coupled with apoptosis induction, as shown by Annexin V stainings (Fig. 2F–G) and cleavage of the apoptotic proteins PARP and Caspase 3 (Fig. 2H–I), and reduced cell proliferation (Fig. 2K). In contrast, Ucf-101 treatment had no effect on MUL1, UBXN7, or HIF-1α in Saos-2 cells (Fig. 2C, E), likely due to already high levels of MUL1 expression in this cell line. Furthermore, Ucf-101 treatment did not induce apoptosis, nor reduce proliferation, in Saos-2 cells (Fig. 2F–H, J–K). These data support a tumor suppressive role for MUL1 specifically in aggressive osteosarcoma cells.

### *3.4. MUL1 E3 ligase activity induces apoptosis and reduces proliferation and migration in 143B cells*

In order to understand whether the effects on cell proliferation and apoptosis in 143B cells directly rely on MUL1 upregulation, as well as on its E3 ligase activity, we transfected 143B cells with a MUL1-overexpressing GFP-MUL1 vector (pMUL1), a GFP vector carrying an E3 ligase-deficient mutant (pMUL1 C/A), or an empty control EGFP vector (pEGFP). Overexpression of wild-type MUL1 significantly reduced UBXN7 and HIF-1α protein levels compared to the results observed in pEGFP-transfected cells (Fig. 3A–B); this was accompanied by increased Annexin V positivity (Fig. 3C–D), cleavage of PARP and Caspase 3 (Fig. 3E–F), as well as reduced cell proliferation rate (Fig. 3G) and migration (Fig. 3H–I). These modulations were absent in cells overexpressing the inactive ligase (MUL1 C/A) (Fig. 3), suggesting that MUL1 E3 ubiquitin ligase activity, and the resulting downregulation of UBXN7 and HIF-1α, are required to exert tumor suppressive function.

### *3.5. Induction of cell death in MUL1-overexpressing osteosarcoma cells is dependent on HIF-1α reduction*

We next assessed whether MUL1-induced cell death depends on HIF-1α inhibition. We treated the transfected 143B cells with HIF-1α inhibitors Chetomin and Echinomycin. In pEGFP and pMUL1 C/A transfected cells, Chetomin reduced HIF-1α to levels observed in pMUL1-cells, inducing apoptosis and reducing cell proliferation (Fig. 4A–B, E–F left panels); Echinomycin did not affect HIF-1α protein levels, consistent with its mechanism of action targeting HIF-1α DNA-binding activity [28]; however, it still induced apoptosis and reduced proliferation (Fig. 4C–D, E–F right panels). In contrast, neither inhibitor exerted additional effects in 143B overexpressing wild-type MUL1, as HIF-1α was already suppressed (Fig. 4A–B, E–F left panels for Chetomin; Fig. 4C–D, E–F right panels for Echinomycin). These results indicate that the tumor-suppressive effects of MUL1 could be mediated by HIF-1α downregulation.

### *3.6. MUL1 deficiency causes an increased tumor phenotype and drug resistance in low aggressive osteosarcoma cells*

Our data highlights a tumor suppressor role for MUL1 in osteosarcoma, raising the possibility that MUL1 loss contributes to the progression of osteosarcoma to a metastatic phenotype. To test this, we generated MUL1 knock-out (KO) Saos-2 cells using the CRISPR-Cas9 system, as previously described [20]. As expected from our previous studies in HEK293 cells [17,18], Saos-2 cells depleted of MUL1 (MUL1 −/−) are characterized by high levels of UBXN7 and HIF-1α expression, with no detectable modulation of HTRA2 levels (Fig. 5A–B). MUL1 loss also enhanced proliferation rate (Fig. 5C) and migration (Fig. 5D–E).

Depletion of MUL1 also conferred resistance to cisplatin: in fact, it was not able to induce apoptosis (Fig. 6A–C), nor reduce the proliferation rate (Fig. 6D), at the standard concentration. Methotrexate had also reduced effects in the absence of MUL1 (Fig. 6E–H). Taken together, our data demonstrate that MUL1 loss in osteosarcoma promotes tumor growth, resistance to anti-proliferative stimuli, and most importantly resistance to chemotherapy, likely through the activation of HIF-1α-related pathways.

### *3.7. MUL1 is required for the canonical mechanisms of regulation of HIF-1α*

To investigate how different levels of MUL1 in osteosarcoma influence the canonical regulatory mechanisms of HIF-1α (hypoxia and ubiquitination), we treated both MUL1-overexpressing 143B cells and MUL1 KO Saos-2 cells with cobalt chloride to mimic the hypoxia conditions or with the proteasome inhibitor carfilzomib (CFZ). Initially, we performed concentration-response experiments to determine the optimal drug concentrations required to increase HIF-1α levels (Fig. S3). Treatment with 100 μM cobalt chloride caused only a slight accumulation of HIF-1α protein levels in pEGFP and pMUL1 C/A 143B cells that express lower levels of MUL1 (Fig. 7A–B). In contrast, in pMUL1 143B cells bearing lower levels of HIF-1α, hypoxia-mimicking conditions led to a greater increase in HIF-1α (Fig. 7A–B). This effect was also observed in Saos-2 MUL1(+/+) cells but, interestingly, not in MUL1(−/−) cells (Fig. 7C–D). These data are consistent with our previous observations in HEK293 cells under hypoxia [17,18], and suggest that MUL1 protein levels are required for hypoxia-mediated HIF-1α degradation. This process appears to depend on HIF-1α ubiquitination: treatment with 50 nM of CFZ slightly increased HIF-1α protein levels in pEGFP and pMUL1 C/A 143B cells (Fig. 7E–F). However, when MUL1 was overexpressed, CFZ treatment strongly enhanced the protein expression of HIF-1α (Fig. 7E–F). Even at a lower concentration (25 nM), which had no effect on pEGFP and pMUL1 C/A cells, CFZ was able to significantly increase HIF-1α levels in pMUL1-transfected cells (Fig. S4A–B). UBXN7 protein levels were similarly affected by CFZ (Fig. 7E–F), suggesting that HIF-1α regulation occurs through the MUL1/UBXN7/HIF-1α axis. In Saos-2 cells, CFZ treatment increased HIF-1α only in MUL1(+/+) cells, with no effects observed in MUL1(−/−) cells (Fig. 7G–H). Once again, UBXN7 protein levels mirrored those of HIF-1α, supporting a direct regulation (Fig. 7G–H). Our data indicate that functional MUL1 expression is required for HIF-1α ubiquitination and proteasomal degradation, highlighting the role of MUL1 and its modulation of

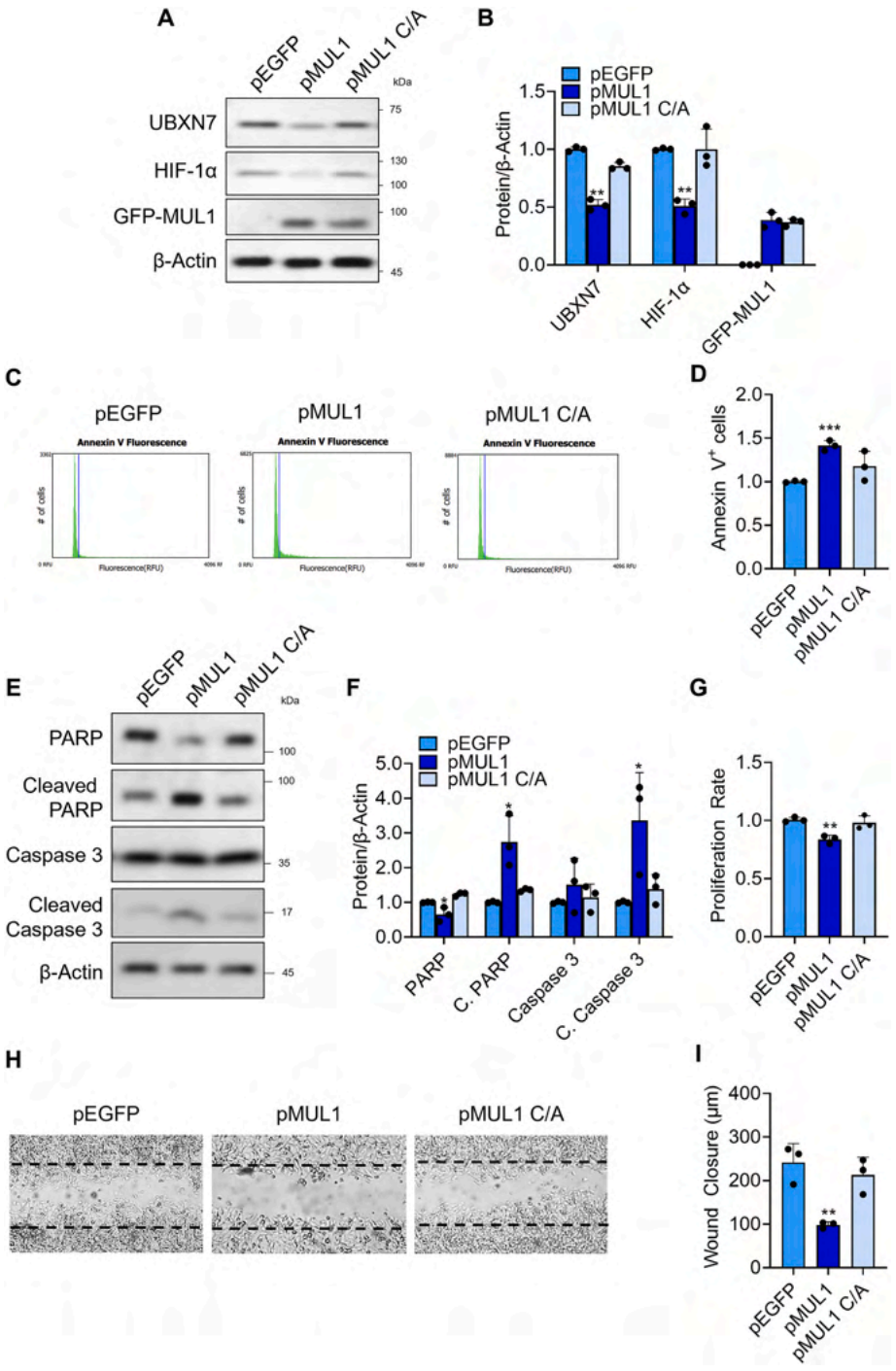


**Fig. 3.** Effects of MUL1 overexpression in 143B cells. Protein expression of the components of the MUL1/HIF-1α pathway in 143B cells transfected with empty vector (pEGFP), GFP-MUL1 (pMUL1) vector and inactive GFP-MUL1 (pMUL1 C/A) vector. A) Western Blot analysis showing the protein levels of GFP-MUL1, UBXN7 and HIF-1α. B) Densitometric analysis of the protein bands normalized against β-Actin. Results are expressed as means ± S.D. of four independent experiments. C) Annexin V staining measured by Tali Apoptosis Kit. D) Quantification of Annexin V+ cells. E) Western Blot analysis showing the protein levels of PARP and Caspase 3, as well as their cleaved forms. F) Densitometric analysis of the protein levels from (E) normalized against β-Actin. G) Cellular proliferation was measured using the CCK8 kit. H) Cell migration was assessed by scratch assay. Representative pictures and I) quantification of wound closure of pEGFP, pMUL1, pMUL1 C/A 143B cells. In D, F–G, I) results are presented as mean ± S.D. of three independent experiments. *$p < 0.05$, **$p < 0.01$ and ***$p < 0.0001$ *vs* pEGFP transfected cells.

UBXN7 levels, as a critical component of the canonical HIF-1α degradation pathway.

### 3.8. *MUL1 levels regulate metabolism in osteosarcoma cells*

Since our previous studies identified a key function for MUL1 as a regulator of metabolism, and considering that metastatic osteosarcoma cells exhibit a classical Warburg effect [29], we evaluated the metabolic activity of the MUL1-overexpressing or the MUL1-KO osteosarcoma cell lines, to determine whether different MUL1 levels influence cell metabolism. Consistent with our previous studies in HEK293 cells [17–19] and the reduction of HIF-1α detected in osteosarcoma cells expressing high levels of MUL1, Seahorse analyses showed that MUL1 overexpression in 143B significantly decreased both glycolytic and

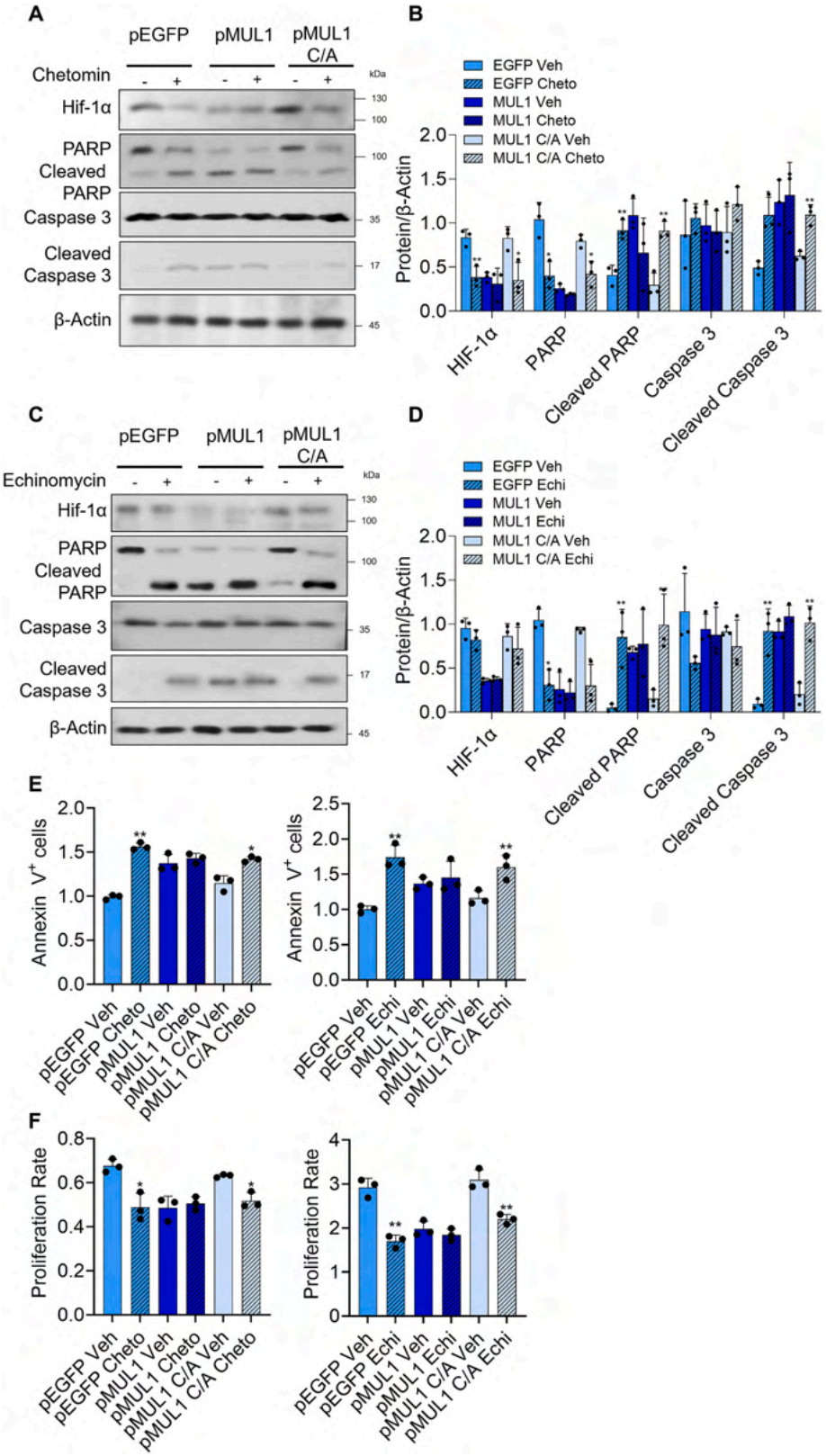


**Fig. 4.** Effects of HIF-1α inhibitors on transfected 143B cells. pEGFP-, pMUL1- and pMUL1 C/A-transfected cells were treated with the Chetomin (50 nM) and Echinomycin (20 nM) or DMSO as vehicle (Veh) for 24 h. A) Western Blot analysis showing the protein levels of PARP and Caspase 3, as well as their cleaved forms, of the Chetomin-treated cells. B) Densitometric analysis of the protein levels from (B) normalized against β-Actin. C) Western Blot analysis showing the protein levels of PARP and Caspase 3, as well as their cleaved forms, of the Echinomycin-treated cells. D) Densitometric analysis of the protein levels from (C) normalized against β-Actin. E) Quantification of Annexin V+ cells, obtained with the Tali Apoptosis Kit, of both treatments. F) Cellular proliferation was measured using the CCK8 kit. All results are presented as mean ± S.D. of three independent experiments. *$p < 0.05$ and **$p < 0.01$ *vs* respective cells treated with vehicle (Veh).

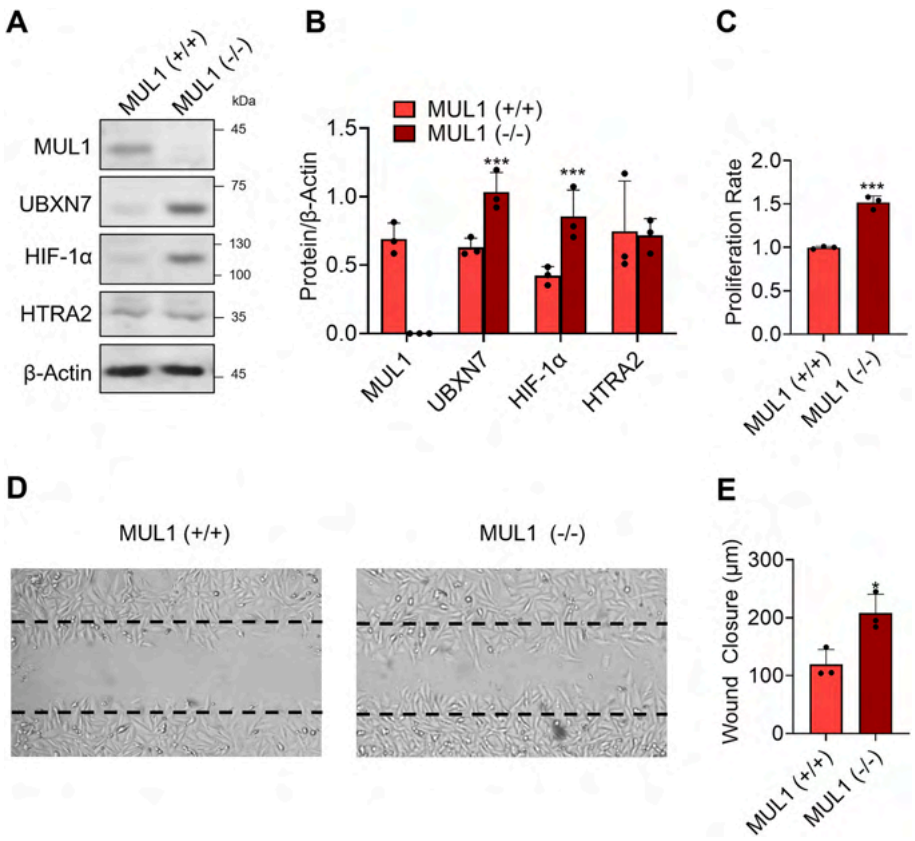


**Fig. 5.** Effects of MUL1 CRISPR-KO in Saos-2 osteosarcoma cell line. A) Western Blot analysis showing the protein levels of MUL1, UBXN7, HIF-1α and HTRA2 in control Saos-2 cells [MUL1(+/+)] and MUL1 CRISPR-KO Saos-2 cells [MUL1(−/−)]. B) Densitometric analysis of the protein levels from (A) normalized against β-Actin. C) Cellular proliferation evaluated by the CCK8 kit. D) Cell migration was assessed by scratch assay. Representative picture and E) Quantification of wound closure of MUL1(+/+) and MUL1(−/−) cells. All results are presented as mean ± S.D. of three independent experiments. *p < 0.05 and ***p < 0.0001 *vs* MUL1(+/+).

compensatory glycolysis capacities (Fig. 8A–B). This shift may explain the reduced cell proliferation and increased apoptosis observed with MUL1 expression.

Furthermore, MUL1 overexpression enhanced mitochondrial metabolism (Fig. 8C–D) and OXPHOS became the main source of ATP, compared to pEGFP and pMUL1 C/A transfected cells (Fig. 8D). Despite observing a strong reduction of the overall ATP production, we report a trend of increase in mitochondrial respiration and mitochondrial ATP generation (Fig. 8C–D), consistent with the increased levels of MUL1. MUL1-overexpressing 143B cells displayed a less aggressive metabolic profile, characterized by attenuation of the Warburg effect. Conversely, MUL1 knock out in Saos-2 cells induced the opposite phenotype. MUL1 (−/−) cells showed enhanced glycolytic capacity at both basal and compensatory level (Fig. 8E–F), the hallmark of more aggressive osteosarcomas. These cells became more reliant on glycolysis for their ATP needs, with reduced OXPHOS-dependent ATP generation (Fig. 8G), mitochondrial respiration, and mitochondrial ATP production (Fig. 8H). The overall metabolic phenotype of MUL1(−/−) Saos-2 cells resembled that of highly aggressive osteosarcoma cell lines, such as 143B [29].

### *3.9. HIF1-α inactivation partially rescues the phenotype induced by MUL1-KO*

In order to further verify whether increased aggressiveness and glycolysis observed in osteosarcoma are dependent on the MUL1/HIF-1α pathway, we inhibited HIF-1α in MUL1-overexpressing or in MUL1-KO osteosarcoma cell lines. HIF-1α downregulation by siRNA in pEGFP-, pMUL1- and pMUL1 C/A-143B cells reduced the expression of HIF-1α by roughly 50 % (Fig. 9A–B); this reduction of HIF-1α was coupled with the decrease of both proliferation (Fig. 9C) as well as basal and compensatory glycolysis (Fig. 9D) in pEGFP- and pMUL1 C/A-cells; in pMUL1 cells, siRNA treatment led to a trend of further reduction of proliferation and glycolysis (Fig. 9A–D). In Saos-2, HIF-1α silencing in MUL1(−/−) cells reduced the protein levels of HIF-1α to control values (Fig. 9E–F). This reduction was also accompanied by a significant decrease of cell proliferation (Fig. 9G) as well as in basal and compensatory glycolysis (Fig. 9H). Nonetheless, the levels of proliferation and metabolism remained higher compared with control MUL1(+/+) cells (Fig. 9G–H), indicating a partial rescue of the phenotype induced by MUL1 inactivation. These data were partially confirmed when HIF-1α was inhibited using the small molecule PX-478. Indeed, in 143B pEGFP and pMUL1 C/A cells, PX-478 reduced the protein levels of HIF-1α, with a consequent reduction in proliferation and glycolysis (Fig. S5A–D). As shown in Fig. 4, using other HIF-1α inhibitors, the effects were not observed in pMUL1 cells, where HIF-1α was not further reduced. Instead, in Saos-2 cells, PX-478 treatment mirrored the results obtained with siRNA (Fig. S5E–H), where HIF-1α inhibition in MUL1(−/−) cells partially rescued their phenotype in terms of proliferation and glycolysis. Altogether, our data support the role of HIF-1α and its expression in the effects of MUL1 inactivation.

## 4. Discussion

The metastatic process ultimately determines the clinical outcome of osteosarcoma. However, the molecular mechanisms driving metastasis in osteosarcoma are not yet fully clarified [5,30]. Given the intrinsic radioresistance of osteosarcoma and the limited benefit of surgical resection once metastasis occurs, chemotherapy represents a valid

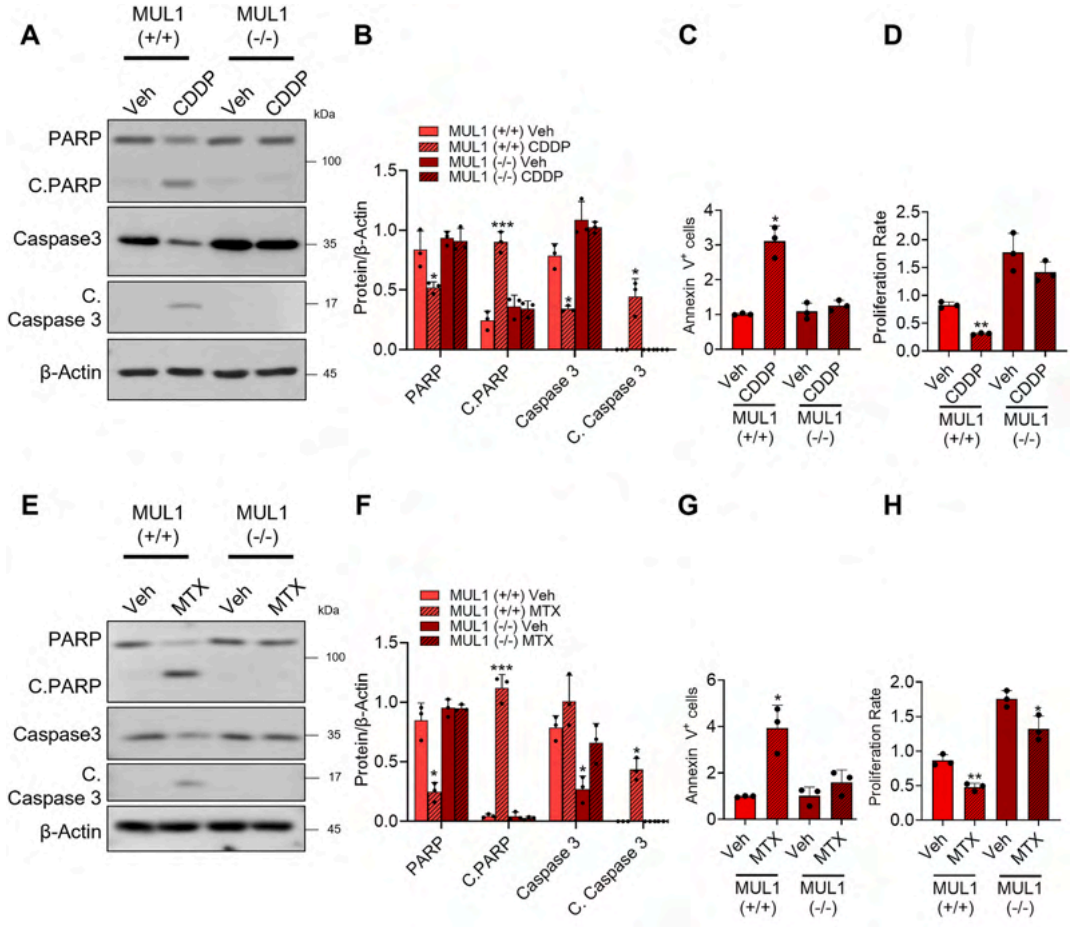


**Fig. 6.** Effects of cisplatin and methotrexate on MUL1 CRISPR-KO Saos-2 cells. A) Western Blot analysis showing the protein levels of PARP and Caspase 3, as well as their cleaved (C.) forms, upon treatment with 2 μM cisplatin (CCDP) or DMSO as Vehicle (Veh) for 24 h. B) Densitometric analysis of the protein levels from (A) normalized against β-Actin. C) Quantification of Annexin V+ cells, obtained with the Tali Apoptosis Kit. D) Cellular proliferation measured using the CCK8 kit. E) Western Blot analysis showing the protein levels of PARP and Caspase 3, as well as their cleaved (C.) forms, upon treatment with 100 nM methotrexate (MTX) or DMSO as Vehicle (Veh) for 5 days. F) Densitometric analysis of the protein levels from (E) normalized against β-Actin. G) Quantification of Annexin V+ cells, obtained with the Tali Apoptosis Kit. H) Cellular proliferation measured using the CCK8 kit. All results are presented as mean ± S.D. of three independent experiments. *p < 0.05, **p < 0.001 and ***p < 0.0001 *vs* respective cells treated with vehicle (Veh).

treatment option [31]. Nevertheless, metastasis in osteosarcoma is often associated with resistance to the current chemotherapeutic regimen, cisplatin, doxorubicin, methotrexate, and ifosfamide [31]. In this work, our data highlights a potential therapeutic approach based on MUL1 induction and consequent HIF-1α downregulation. HIF-1α is known to enhance the metastatic potential in several cancers, including breast, lung, liver metastasis of colorectal cancer, and clear renal cell carcinoma [32–36]. In osteosarcoma, HIF-1α-regulated genes containing Hypoxia-Responsive Elements (HRE) promote metastasis by inhibiting apoptosis, inducing angiogenesis *via* Vascular Endothelial Growth Factor (VEGF) expression, enhancing glycolysis through metabolic reprogramming, and activating EMT [37–41]. Thus, HIF-1α plays a key role in osteosarcoma metastasis by increasing invasiveness, bolstering the survival potential, stimulating vascular remodeling, and reducing cell adhesion through EMT [13,42]. On these bases, HIF-1α downregulation not only triggers apoptosis, as previously shown *in vitro*, but can also impair metastatic progression [14,43]. Unfortunately, direct targeting of HIF-1α in osteosarcoma has been challenging. Agents such as Echinomycin have shown limited efficacy in clinical trials, and small-molecule inhibitors still need to be tested in this context [44,45]. We previously demonstrated in HEK293 cells that MUL1 regulates HIF-1α *via* a pathway downstream of the $CRL2^{VHL}$ complex and by hypoxia, with direct effects on cell metabolism [17,18]. To date, this pathway has not been studied in osteosarcoma. Indeed, although the role of HIF-1α signaling and its regulation in osteosarcoma are well-documented [13], and despite MUL1 having been investigated in other cancers, both as an E3 ubiquitin ligase [22] and as a SUMO E3 ligase [46], the interactions between MUL1, UBXN7 and HIF-1α have never been explored or evaluated. A recent study reported a direct interaction between MUL1 and HIF-2α, which was disrupted in clear renal cell carcinoma and resulted in a similar metabolic phenotype [47]. However, that mechanism was distinct and did not depend on the regulation mediated by the MUL1-UBXN7 axis. Here, we show for the first time that the MUL1/UBXN7/HIF-1α pathway is disrupted in metastatic osteosarcoma: metastatic cell lines display reduced MUL1 expression, which correlates with increased UBXN7 and HIF-1α levels and with glycolysis-dependent metabolism [29]. The regulation of MUL1 protein expression involves a finely regulated mechanism, as in 143B cells reduced MUL1 protein levels does not depend on decreased RNA expression, but may instead be related to post-transcriptional regulation (for instance due to the intervention of miRNAs) or post-translational modifications. In fact, the mechanism of MUL1 inactivation in 143B cells may also involve HTRA2 hyperactivation, since its inhibition is able to increase MUL1 levels in 143B cells, but not in Saos-2. These data are consistent with our observations in the patient datasets, and with previous reports identifying HTRA2 as an oncogene in several cancers and as a marker of poor prognosis in lymphoma, breast, ovarian, germ cell, and prostate cancers [48]. Thus, high HTRA2 and low MUL1 expression, associated with reduced survival

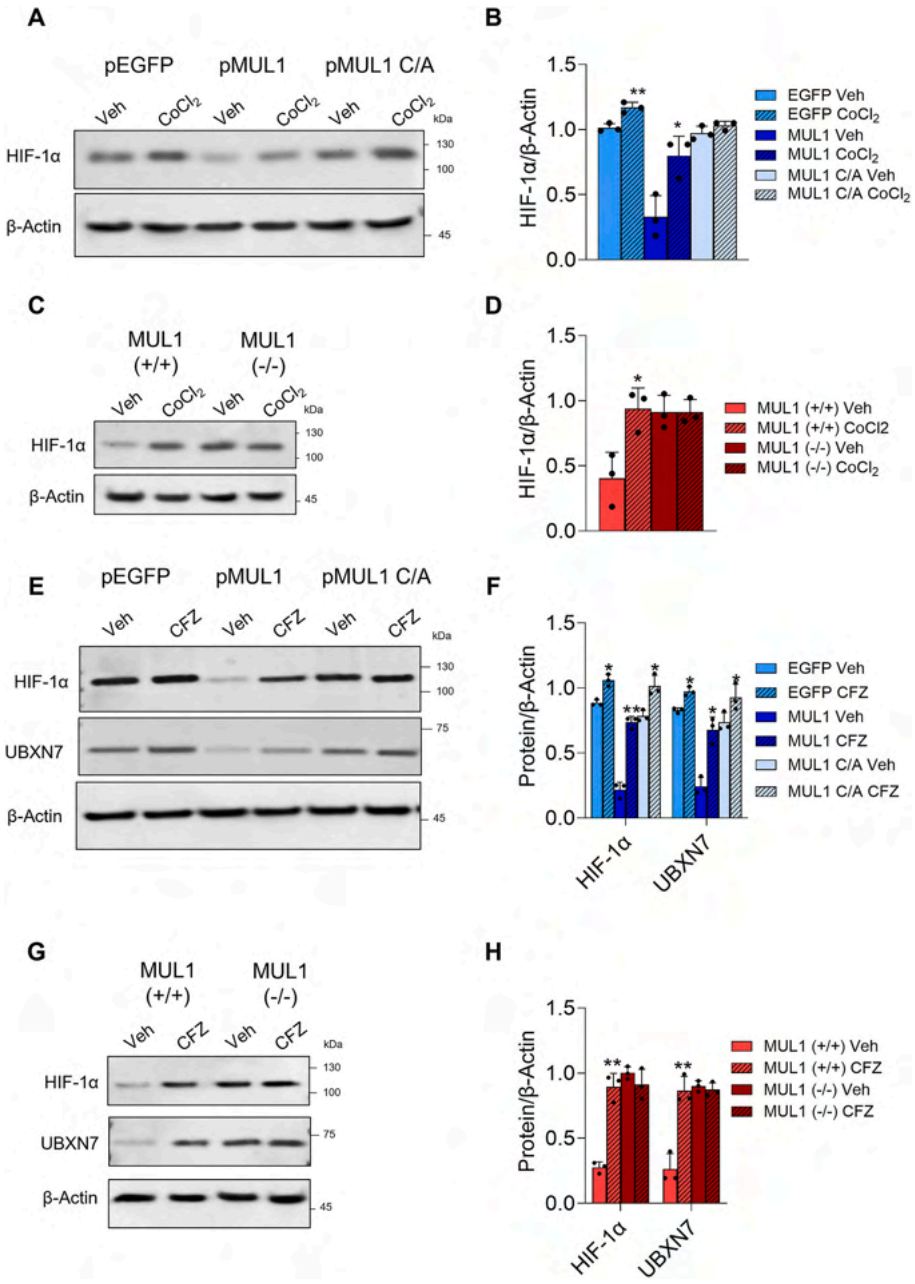


**Fig. 7.** Effects of cobalt chloride and carfilzomib on osteosarcoma cell lines. 143B and Saos-2 cells were treated with cobalt chloride (CoCl2) at 100 μM for 6 h or with carfilzomib (CFZ) at 50 nM for 4 h. A) Western Blot and B) densitometrical analysis normalized against β-Actin of the protein levels of HIF-1α in pEGFP, pMUL1 and pMUL1 C/A 143B cells treated with CoCl2 or DMSO as vehicle (Veh). C) Western Blot and D) densitometrical analysis normalized against β-Actin of the protein levels of HIF-1α in MUL1(+/+) and MUL1(−/−) Saos-2 cells treated with CoCl2 or DMSO as vehicle (Veh). E) Western Blot and F) densitometrical analysis normalized against β-Actin of the protein levels of HIF-1α and UBXN7 in pEGFP, pMUL1 and pMUL1 C/A 143B cells treated with CFZ at 50 nM, or DMSO as vehicle (Veh). G) Western Blot and H) densitometrical analysis normalized against β-Actin of the protein levels of HIF-1α and UBXN7 in MUL1(+/+) and MUL1(−/−) Saos-2 cells treated with CFZ at 50 nM or DMSO as vehicle (Veh). All results are presented as mean ± S.D. of three independent experiments. *$p < 0.05$ and **$p < 0.001$ *vs* respective cells treated with vehicle (Veh).

in osteosarcoma patients, may reflect this regulatory interaction [49–52]. Importantly, our data suggest that MUL1 loss is a key event in osteosarcoma progression and metastasis. The increase of proliferation rate, migration and the resistance to cisplatin and methotrexate caused by MUL1 downregulation could be dependent on the increased levels of HIF-1α (through the accumulation of UBXN7), potentially reflected in increased survival, resistance to apoptosis and EMT activation [11]. This metastatic shift also involved an increase in glycolytic capacity, at the expense of OXPHOS, observed in the absence of MUL1. This classical Warburg effect is responsible for increasing the metastatic capacity of osteosarcoma cells, as well as increasing the proliferation capacity and drug resistance, as seen both *in vivo* and *in vitro* [10,53]. Therefore, downregulating MUL1 could be a key molecular event that leads to metabolic reprogramming in osteosarcoma. Conversely, restoring MUL1 expression in aggressive osteosarcoma cells reduced glycolytic capacity and enhanced apoptosis, consistently with previous findings [10]. These effects appear to directly depend on HIF-1α inhibition, as no synergistic effects were observed when MUL1 overexpression was combined with pharmacological HIF-1α inhibitors. In this regard, MUL1 induction could represent a starting point for the development of a new

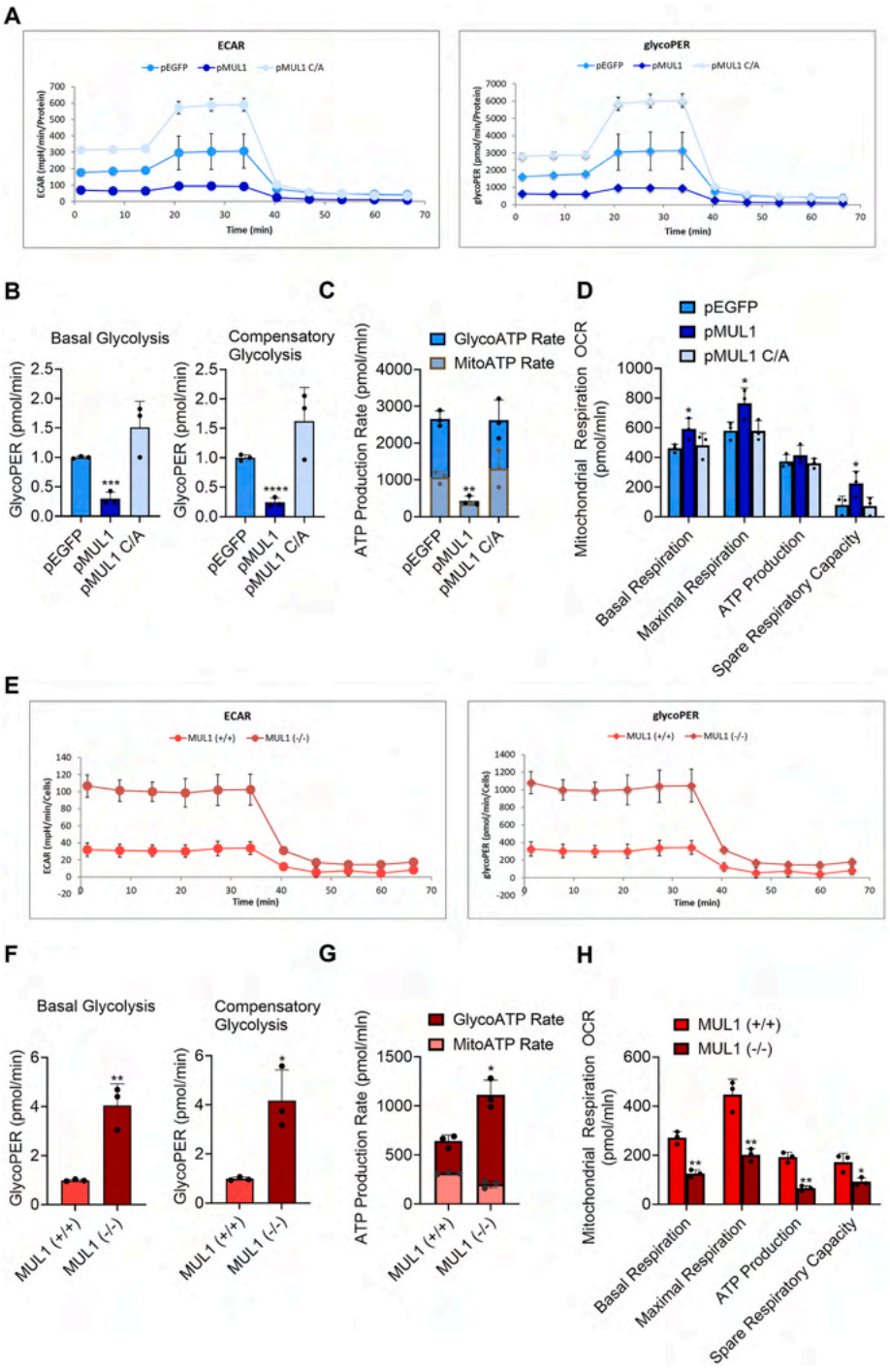


**Fig. 8.** Effects of MUL1 overexpression and knockout in osteosarcoma cell lines on cell metabolism. A) Glycolytic capacity of the 143B cells was assessed using the glycolytic rate assay. Extracellular acidification rate (ECAR) and glycolysis' Proton Efflux Rate (glycoPER) was measured using the Seahorse extracellular flux analyzer. 143B cells were transfected with pEGFP empty vector, pGFP-MUL1 vector or pMUL1 C/A vector. B) Quantification of basal and compensatory glycolysis of the transfected 143B cells. C) ATP production rate measured using the real-time ATP Rate Assay. Mitochondrial and glycolytic ATP production in the cells was determined. D) Mitochondrial respiration was monitored using the Mitochondrial Stress Test kit. Basal respiration, maximal respiration, ATP production and spare respiratory capacity were quantified. In B–D) results are presented as mean ± S.D. of three independent experiments. *$p < 0.05$, **$p < 0.001$, ***$p < 0.0001$ and ****$p < 00001$ *vs* pEGFP-transfected cells. E) ECAR and glycoPER, F) Quantification of basal and compensatory glycolysis, G) ATP production rate, H) mitochondrial respiration of MUL1(+/+) Saos-2 cells and MUL1(−/−) Saos-2 cells. In F–H) results are presented as mean ± S.D. of three independent experiments. *$p < 0.05$ and **$p < 0.001$ *vs* MUL1(+/+).

therapeutic strategy aimed at metabolic reprogramming in metastatic osteosarcoma. Nevertheless, important questions remain to be addressed. The precise molecular mechanisms regulating MUL1 inactivation and the potential involvement of other MUL1 targets in the metastasis of osteosarcoma still need to be investigated: in this regard, the partial rescue of the phenotype caused by MUL1 inactivation by HIF-1α silencing suggests that other MUL1 substrates, that may act as oncogenes in osteosarcoma, appear to be involved in the increase of glycolysis and proliferation caused by MUL1 loss. Moreover, while MUL1 functions as a tumor suppressor in osteosarcoma, it may act as an

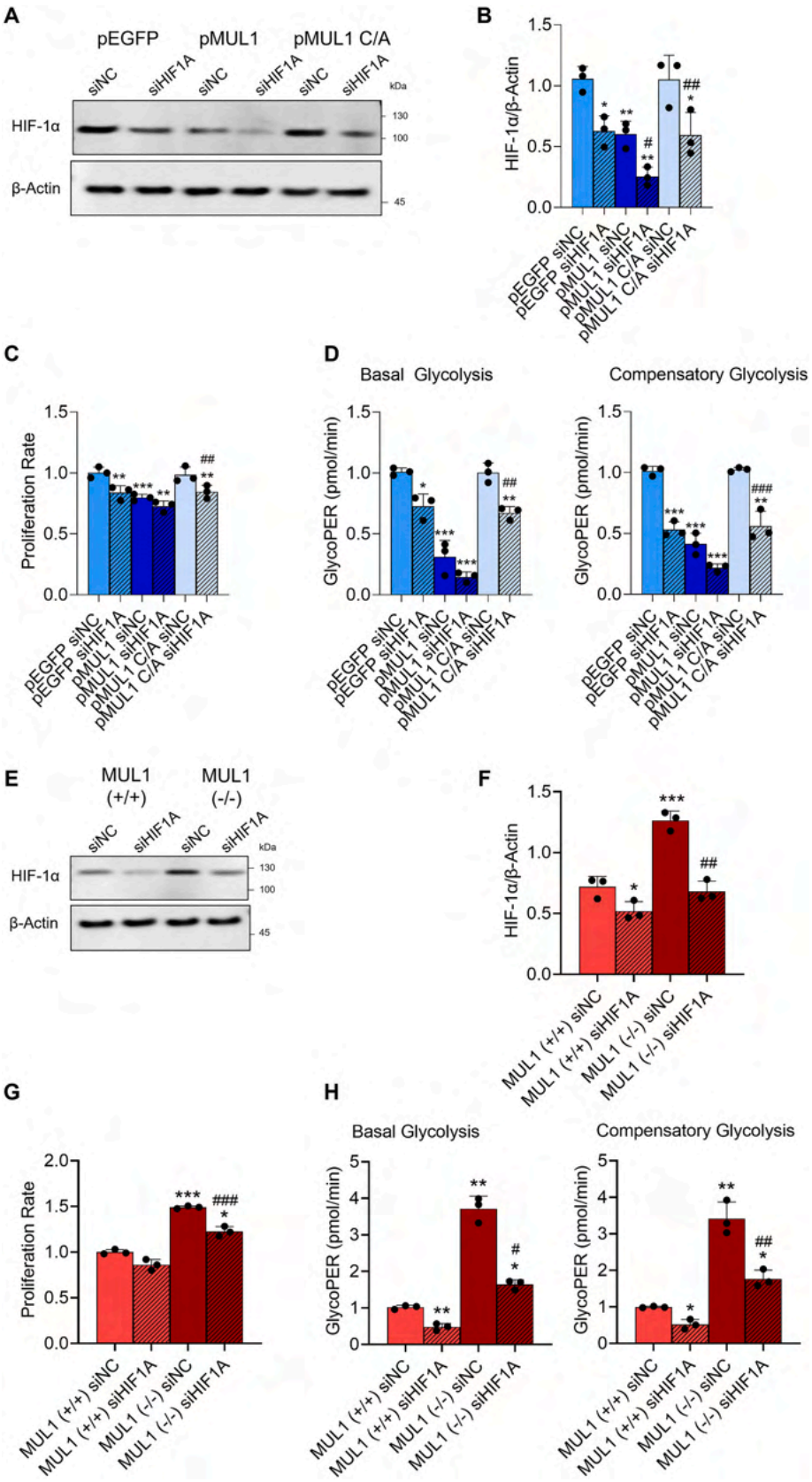


*(caption on next page)*

**Fig. 9.** Rescue experiments with HIF-1α siRNA. A) Western Blot and B) densitometrical analysis normalized against β-Actin of the protein levels of HIF-1α in pEGFP, pMUL1 and pMUL1 C/A 143B cells transfected with negative control siRNA (siNC) or siRNA directed against HIF1A (siHIF1A). C) Cellular proliferation measured using the CCK8 kit. D) Quantification of Basal and Compensatory glycolysis of the transfected 143B cells, obtained by Seahorse Glycolytic Rate assay. In B–D) results are presented as mean ± S.D. of three independent experiments. *$p < 0.05$, **$p < 0.001$ and ***$p < 0.0001$ *vs* pEGFP-siNC transfected cells; $^{\#}p < 0.05$, $^{\#\#}p < 0.001$ and $^{\#\#\#}p < 0.0001$ *vs* respective siNC-treated cells. E) Western Blot and F) densitometrical analysis normalized against β-Actin of the protein levels of HIF-1α in MUL1(+/+) Saos-2 cells and MUL1(−/−) Saos-2 cells transfected with negative siNC or siHIF1A. G) Cellular proliferation measured using the CCK8 kit. H) Quantification of basal and compensatory glycolysis of the transfected Saos-2 cells, obtained by Seahorse Glycolytic Rate assay. In F–H) results are presented as mean ± S.D. of three independent experiments. *$p < 0.05$, **$p < 0.001$ and ***$p < 0.0001$ *vs* MUL1(+/+) siNC cells; $^{\#}p < 0.05$, $^{\#\#}p < 0.001$, and $^{\#\#\#}p < 0.0001$ *vs* MUL1 (−/−) siNC cells.

oncogene in other cancers [22]. This context-dependent role likely reflects differential regulation and expression of its substrates, thus suggesting that targeting multiple components of the MUL1-UBXN7-HIF-1α pathway may be a more effective therapeutic approach.

In summary, we describe for the first time a tumor-suppressive role for MUL1 in osteosarcoma. MUL1 induction reduces HIF-1α levels, reprograms metabolism, and enhances apoptosis in aggressive osteosarcoma cells. However, *in vivo* studies and an in-depth analysis of the molecular mechanisms of MUL1 inactivation in aggressive osteosarcoma, as well as studies focusing on the involvement of other MUL1 substrates, will be necessary in order to strengthen the role of MUL1 as a therapeutic target in this type of cancer.

## CRediT authorship contribution statement

**Jacopo Di Gregorio:** Writing – original draft, Visualization, Validation, Methodology, Investigation, Formal analysis, Conceptualization. **Sara Terreri:** Methodology, Formal analysis. **Michela Rossi:** Writing – review & editing, Visualization, Validation, Methodology, Formal analysis, Conceptualization. **Giulia Battafarano:** Validation, Formal analysis. **Laura Di Giuseppe:** Validation, Formal analysis. **Olivia Pagliarosi:** Validation, Formal analysis. **Lucia Cilenti:** Writing – review & editing, Validation. **Enrico Ricevuto:** Writing – review & editing, Validation. **Antonis S. Zervos:** Writing – review & editing, Supervision, Resources, Conceptualization. **Vincenzo Flati:** Writing – review & editing, Writing – original draft, Supervision, Resources, Project administration, Funding acquisition, Data curation, Conceptualization. **Andrea Del Fattore:** Writing – review & editing, Writing – original draft, Supervision, Software, Resources, Project administration, Funding acquisition, Data curation, Conceptualization.

## Funding

JDG, ST and MR are supported by Fondazione Umberto Veronesi. This work was also supported by the Italian Ministry of Health with the "Current Research funds" (to ADF), by the intramural "DISCAB GRANT 2024" (code 07_DG_2024_03 to VF) awarded by the Department of Biotechnological, and Applied Clinical Sciences, University of L'Aquila, and by the "Progetto di ricerca di Ateneo per la ricerca di base 2024" (code 07_PROGETTI_ATENEO_2024 to VF).

## Declaration of competing interest

The authors declare no competing interests.

## Acknowledgements

We thank Cristina Ciamarone for the graphical abstract artwork.

## Appendix A. Supplementary data

Supplementary data to this article can be found online at https://doi.org/10.1016/j.bbamcr.2025.120101.

## Data availability

The data that support the findings of this study are available from the corresponding author upon request.

## References

[1] L.R. Sadykova, A.I. Ntekim, M. Muyangwa-Semenova, C.S. Rutland, J. N. Jeyapalan, N. Blatt, et al., Epidemiology and risk factors of osteosarcoma, Cancer Investig. 38 (5) (2020) 259–269, https://doi.org/10.1080/07357907.2020.1768401 (Epub 20200601. PubMed PMID: 32400205).

[2] S.A. Eccles, D.R. Welch, Metastasis: recent discoveries and novel treatment strategies, Lancet 369 (9574) (2007) 1742–1757, https://doi.org/10.1016/s0140-6736(07)60781-8 (PubMed PMID: 17512859; PubMed Central PMCID: PMC2214903).

[3] F. Eilber, A. Giuliano, J. Eckardt, K. Patterson, S. Moseley, J. Goodnight, Adjuvant chemotherapy for osteosarcoma: a randomized prospective trial, J. Clin. Oncol. 5 (1) (1987) 21–26, https://doi.org/10.1200/jco.1987.5.1.21 (PubMed PMID: 3543236).

[4] A.M. Hong, S. Millington, V. Ahern, G. McCowage, R. Boyle, M. Tattersall, et al., Limb preservation surgery with extracorporeal irradiation in the management of malignant bone tumor: the oncological outcomes of 101 patients, Ann. Oncol. 24 (10) (2013) 2676–2680, https://doi.org/10.1093/annonc/mdt252 (Epub 20130712. PubMed PMID: 23852310).

[5] L. Marchandet, M. Lallier, C. Charrier, M. Baud'huin, B. Ory, F. Lamoureux, Mechanisms of resistance to conventional therapies for osteosarcoma, Cancers (Basel) 13 (4) (2021), https://doi.org/10.3390/cancers13040683 (Epub 20210208. PubMed PMID: 33567616; PubMed Central PMCID: PMC7915189).

[6] D. Wang, X. Niu, Z. Wang, C.L. Song, Z. Huang, K.N. Chen, et al., Multiregion sequencing reveals the genetic heterogeneity and evolutionary history of osteosarcoma and matched pulmonary metastases, Cancer Res. 79 (1) (2019) 7–20, https://doi.org/10.1158/0008-5472.Can-18-1086 (Epub 20181102. PubMed PMID: 30389703).

[7] Y. Zhou, D. Yang, Q. Yang, X. Lv, W. Huang, Z. Zhou, et al., Single-cell RNA landscape of intratumoral heterogeneity and immunosuppressive microenvironment in advanced osteosarcoma, Nat. Commun. 11 (1) (2020) 6322, https://doi.org/10.1038/s41467-020-20059-6 (Epub 20201210. PubMed PMID: 33303760; PubMed Central PMCID: PMC7730477).

[8] R. Ge, G.M. Huang, Targeting transforming growth factor beta signaling in metastatic osteosarcoma, J. Bone Oncol. 43 (2023) 100513, https://doi.org/10.1016/j.jbo.2023.100513 (Epub 20231108. PubMed PMID: 38021074; PubMed Central PMCID: PMC10666000).

[9] Z.X. Chong, S.K. Yeap, W.Y. Ho, Unraveling the roles of miRNAs in regulating epithelial-to-mesenchymal transition (EMT) in osteosarcoma, Pharmacol. Res. 172 (2021) 105818, https://doi.org/10.1016/j.phrs.2021.105818 (Epub 20210813. PubMed PMID: 34400316).

[10] F. An, W. Chang, J. Song, J. Zhang, Z. Li, P. Gao, et al., Reprogramming of glucose metabolism: metabolic alterations in the progression of osteosarcoma, J. Bone Oncol. 44 (2024) 100521, https://doi.org/10.1016/j.jbo.2024.100521 (Epub 20240104. PubMed PMID: 38288377; PubMed Central PMCID: PMC10823108).

[11] N. Suzuki, K. Gradin, L. Poellinger, M. Yamamoto, Regulation of hypoxia-inducible gene expression after HIF activation, Exp. Cell Res. 356 (2) (2017) 182–186, https://doi.org/10.1016/j.yexcr.2017.03.013.

[12] W. Cai, H. Yang, The structure and regulation of Cullin 2 based E3 ubiquitin ligases and their biological functions, Cell Div 11 (1) (2016) 7, https://doi.org/10.1186/s13008-016-0020-7.

[13] J. Zhou, F. Lan, M. Liu, F. Wang, X. Ning, H. Yang, et al., Hypoxia inducible factor-1α as a potential therapeutic target for osteosarcoma metastasis, Front. Pharmacol. 15 (2024) 1350187, https://doi.org/10.3389/fphar.2024.1350187 (Epub 20240124. PubMed PMID: 38327979; PubMed Central PMCID: PMC10847273).

[14] F. Lv, R. Du, W. Shang, S. Suo, D. Yu, J. Zhang, HIF-1α silencing inhibits the growth of osteosarcoma cells by inducing apoptosis, Ann. Clin. Lab. Sci. 46 (2) (2016) 140–146 (PubMed PMID: 27098619).

[15] W. Li, M.H. Bengtson, A. Ulbrich, A. Matsuda, V.A. Reddy, A. Orth, et al., Genome-wide and functional annotation of human E3 ubiquitin ligases identifies MULAN, a mitochondrial E3 that regulates the organelle's dynamics and signaling, PLoS One 3 (1) (2008) e1487, https://doi.org/10.1371/journal.pone.0001487.

[16] J. Li, Q. Wei, C. Guo, F. Du, L. Jinhua, M. Biao, et al., Mitochondrial outer-membrane E3 ligase MUL1 ubiquitinates ULK1 and regulates selenite-induced mitophagy, Autophagy 11 (8) (2015) 1216–1229, https://doi.org/10.1080/15548627.2015.1017180.

[17] L. Cilenti, J. Di Gregorio, C.T. Ambivero, T. Andl, R. Liao, A.S. Zervos, Mitochondrial MUL1 E3 ubiquitin ligase regulates Hypoxia Inducible Factor (HIF-1α) and metabolic reprogramming by modulating the UBXN7 cofactor protein, Sci. Rep. 10 (1) (2020) 1609, https://doi.org/10.1038/s41598-020-58484-8.
[18] J. Di Gregorio, L. Cilenti, C.T. Ambivero, T. Andl, R. Liao, A.S. Zervos, UBXN7 cofactor of CRL3KEAP1 and CRL2VHL ubiquitin ligase complexes mediates reciprocal regulation of NRF2 and HIF-1α proteins, Biochim. Biophys. Acta Mol. Cell Res. 1868 (4) (2021) 118963, https://doi.org/10.1016/j.bbamcr.2021.118963.
[19] L. Cilenti, R. Mahar, J. Di Gregorio, C.T. Ambivero, M.E. Merritt, A.S. Zervos, Regulation of metabolism by mitochondrial MUL1 E3 ubiquitin ligase, Front. Cell. Dev. Biol. 10 (2022) 904728, https://doi.org/10.3389/fcell.2022.904728 (Epub 20220629. PubMed PMID: 35846359; PubMed Central PMCID: PMC9277447).
[20] L. Cilenti, J. Di Gregorio, R. Mahar, F. Liu, C.T. Ambivero, M. Periasamy, et al., Inactivation of mitochondrial MUL1 E3 ubiquitin ligase deregulates mitophagy and prevents diet-induced obesity in mice, Front. Mol. Biosci. 11 (2024) 1397565, https://doi.org/10.3389/fmolb.2024.1397565 (Epub 20240425. PubMed PMID: 38725872; PubMed Central PMCID: PMC11079312).
[21] L. Cilenti, C.T. Ambivero, N. Ward, E.S. Alnemri, D. Germain, A.S. Zervos, Inactivation of Omi/HtrA2 protease leads to the deregulation of mitochondrial Mulan E3 ubiquitin ligase and increased mitophagy, Biochim. Biophys. Acta 1843 (7) (2014) 1295–1307, https://doi.org/10.1016/j.bbamcr.2014.03.027 (Epub 20140405.PubMed PMID: 24709290).
[22] J. Di Gregorio, M. Appignani, V. Flati, Role of the mitochondrial E3 ubiquitin ligases as possible therapeutic targets in cancer therapy, Int. J. Mol. Sci. 24 (24) (2023), https://doi.org/10.3390/ijms242417176 (Epub 20231206. PubMed PMID: 38139010; PubMed Central PMCID: PMC10743160).
[23] J. Di Gregorio, L. Di Giuseppe, S. Terreri, M. Rossi, G. Battafarano, O. Pagliarosi, et al., Protein stability regulation in osteosarcoma: the ubiquitin-like modifications and glycosylation as mediators of tumor growth and as targets for therapy, Cells 13 (6) (2024), https://doi.org/10.3390/cells13060537 (Epub 20240318. PubMed PMID: 38534381; PubMed Central PMCID: PMC10969184).
[24] M.L. Kuijjer, H. Rydbeck, S.H. Kresse, E.P. Buddingh, A.B. Lid, H. Roelofs, et al., Identification of osteosarcoma driver genes by integrative analysis of copy number and gene expression data, Genes Chromosom. Cancer 51 (7) (2012) 696–706, https://doi.org/10.1002/gcc.21956 (Epub 20120327. PubMed PMID: 22454324).
[25] A.P. Renjini, S. Titus, P. Narayan, M. Murali, R.K. Jha, M. Laloraya, STAT3 and MCL-1 associate to cause a mesenchymal epithelial transition, J. Cell Sci. 127 (Pt 8) (2014) 1738–1750, https://doi.org/10.1242/jcs.138214 (Epub 20140130. PubMed PMID: 24481815).
[26] S.U. Lauvrak, E. Munthe, S.H. Kresse, E.W. Stratford, H.M. Namløs, L.A. Meza-Zepeda, et al., Functional characterisation of osteosarcoma cell lines and identification of mRNAs and miRNAs associated with aggressive cancer phenotypes, Br. J. Cancer 109 (8) (2013) 2228–2236, https://doi.org/10.1038/bjc.2013.549 (Epub 20130924.PubMed PMID: 24064976; PubMed Central PMCID: PMC3798956.).
[27] D. Su, Z. Su, J. Wang, S. Yang, J. Ma, UCF-101, a novel Omi/HtrA2 inhibitor, protects against cerebral ischemia/reperfusion injury in rats, Anat. Rec. (Hoboken) 292 (6) (2009) 854–861, https://doi.org/10.1002/ar.20910 (PubMed PMID: 19462455).
[28] D. Kong, E.J. Park, A.G. Stephen, M. Calvani, J.H. Cardellina, A. Monks, et al., Echinomycin, a small-molecule inhibitor of hypoxia-inducible factor-1 DNA-binding activity, Cancer Res. 65 (19) (Oct 1 2005) 9047–9055, https://doi.org/10.1158/0008-5472.CAN-05-1235 (PMID: 16204079).
[29] A.H. Giang, T. Raymond, P. Brookes, Bentley K. de Mesy, E. Schwarz, R. O'Keefe, et al., Mitochondrial dysfunction and permeability transition in osteosarcoma cells showing the Warburg effect, J. Biol. Chem. 288 (46) (2013) 33303–33311, https://doi.org/10.1074/jbc.M113.507129 (Epub 20131007. PubMed PMID: 24100035; PubMed Central PMCID: PMC3829176).
[30] G. Sheng, Y. Gao, Y. Yang, H. Wu, Osteosarcoma and metastasis, Front. Oncol. 11 (2021) 780264, https://doi.org/10.3389/fonc.2021.780264 (Epub 20211210. PubMed PMID: 34956899; PubMed Central PMCID: PMC8702962).
[31] A.J. Saraf, J.M. Fenger, R.D. Roberts, Osteosarcoma: accelerating progress makes for a hopeful future, Front. Oncol. 8 (2018) 4, https://doi.org/10.3389/fonc.2018.00004 (Epub 20180126. PubMed PMID: 29435436; PubMed Central PMCID: PMC5790793).
[32] J. Zhao, H. Zhang, Y. Liu, G. Lu, Z. Wang, Q. Mo, et al., HIF-1α knockdown suppresses breast cancer metastasis via epithelial mesenchymal transition Abrogation, Heliyon 10 (19) (2024) e37900, https://doi.org/10.1016/j.heliyon.2024.e37900 (Epub 20240914. PubMed PMID: 39386828; PubMed Central PMCID: PMC11462230).
[33] W. Ren, D. Mi, K. Yang, N. Cao, J. Tian, Z. Li, et al., The expression of hypoxia-inducible factor-1α and its clinical significance in lung cancer: a systematic review and meta-analysis, Swiss Med. Wkly. 143 (2013) w13855, https://doi.org/10.4414/smw.2013.13855 (Epub 20130906. PubMed PMID: 24018850).
[34] Y. Wada, Y. Morine, S. Imura, T. Ikemoto, Y. Saito, C. Takasu, et al., HIF-1α expression in liver metastasis but not primary colorectal cancer is associated with prognosis of patients with colorectal liver metastasis, World J. Surg. Oncol. 18 (1) (2020) 241, https://doi.org/10.1186/s12957-020-02012-5.
[35] B. Golijanin, K. Malshy, S. Khaleel, G. Lagos, A. Amin, L. Cheng, et al., Evolution of the HIF targeted therapy in clear cell renal cell carcinoma, Cancer Treat. Rev. 121 (2023) 102645, https://doi.org/10.1016/j.ctrv.2023.102645 (Epub 20231015. PubMed PMID: 37879247).
[36] E.B. Rankin, J.M. Nam, A.J. Giaccia, Hypoxia: signaling the metastatic cascade, Trends Cancer. 2 (6) (2016) 295–304, https://doi.org/10.1016/j.trecan.2016.05.006 (Epub 20160602. PubMed PMID: 28741527; PubMed Central PMCID: PMC5808868).
[37] Y. Zhang, S. Sun, Y. Qi, Y. Dai, Y. Hao, M. Xin, et al., Characterization of tumour microenvironment reprogramming reveals invasion in epithelial ovarian carcinoma, J. Ovarian Res. 16 (1) (2023) 200, https://doi.org/10.1186/s13048-023-01270-7.
[38] M.J. Watson, P.D.A. Vignali, S.J. Mullett, A.E. Overacre-Delgoffe, R.M. Peralta, S. Grebinoski, et al., Metabolic support of tumour-infiltrating regulatory T cells by lactic acid, Nature 591 (7851) (2021) 645–651, https://doi.org/10.1038/s41586-020-03045-2 (Epub 20210215. PubMed PMID: 33589820; PubMed Central PMCID: PMC7990682).
[39] X. Li, Q. Lu, W. Xie, Y. Wang, G. Wang, Anti-tumor effects of triptolide on angiogenesis and cell apoptosis in osteosarcoma cells by inducing autophagy via repressing Wnt/β-Catenin signaling, Biochem. Biophys. Res. Commun. 496 (2) (2018) 443–449, https://doi.org/10.1016/j.bbrc.2018.01.052 (Epub 20180109. PubMed PMID: 29330051).
[40] H. Harjunpää, M. Llort Asens, C. Guenther, S.C. Fagerholm, Cell adhesion molecules and their roles and regulation in the immune and tumor microenvironment, Front. Immunol. 10 (2019) 1078, https://doi.org/10.3389/fimmu.2019.01078 (Epub 20190522. PubMed PMID: 31231358; PubMed Central PMCID: PMC6558418).
[41] X. Wang, Z. Hu, Z. Wang, Y. Cui, X. Cui, Angiopoietin-like protein 2 is an important facilitator of tumor proliferation, metastasis, angiogenesis and glycolysis in osteosarcoma, Am. J. Transl. Res. 11 (10) (2019) 6341–6355 (Epub 20191015. PubMed PMID: 31737187; PubMed Central PMCID: PMC6834488).
[42] H. Feng, J. Wang, W. Chen, B. Shan, Y. Guo, J. Xu, et al., Hypoxia-induced autophagy as an additional mechanism in human osteosarcoma radioresistance, J. Bone Oncol. 5 (2) (2016) 67–73, https://doi.org/10.1016/j.jbo.2016.03.001 (Epub 20160309. PubMed PMID: 27335774; PubMed Central PMCID: PMC4908188.).
[43] G. He, J.J. Nie, X. Liu, Z. Ding, P. Luo, Y. Liu, et al., Zinc oxide nanoparticles inhibit osteosarcoma metastasis by downregulating β-catenin via HIF-1α/BNIP3/LC3B-mediated mitophagy pathway, Bioact. Mater. 19 (2023) 690–702, https://doi.org/10.1016/j.bioactmat.2022.05.006 (Epub 20220513. PubMed PMID: 35600978; PubMed Central PMCID: PMC9112061).
[44] W.J. Gradishar, N.J. Vogelzang, L.J. Kilton, S.J. Leibach, A.W. Rademaker, S. French, et al., A phase II clinical trial of echinomycin in metastatic soft tissue sarcoma. An Illinois Cancer Center Study, Investig. New Drugs 13 (2) (1995) 171–174, https://doi.org/10.1007/bf00872868 (PubMed PMID: 8617582).
[45] R.A. Qannita, A.I. Alalami, A.A. Harb, S.M. Aleidi, J. Taneera, E. Abu-Gharbieh, et al., Targeting hypoxia-inducible factor-1 (HIF-1) in cancer: emerging therapeutic strategies and pathway regulation, Pharmaceuticals 17 (2) (2024) 195, https://doi.org/10.3390/ph17020195 (PubMed PMID).
[46] J. Wu, M. Huang, W. Dong, Y. Chen, Q. Zhou, Q. Zhang, J. Zheng, et al., SUMO E3 ligase MUL1 inhibits lymph node metastasis of bladder cancer by mediating mitochondrial HSPA9 translocation, Int. J. Biol. Sci. 20 (10) (Jul 15 2024) 3986–4006, https://doi.org/10.7150/ijbs.98772.
[47] Z.A. Bacigalupa, E.N. Arner, L.M. Vlach, M.M. Wolf, W.A. Brown, E.S. Krystofiak, X. Ye, et al., HIF-2α expression and metabolic signaling require ACSS2 in clear cell renal cell carcinoma, J. Clin. Invest. 134 (12) (Jun 17 2024) e164249, https://doi.org/10.1172/JCI164249.
[48] L. Wu, X. Li, Z. Li, Y. Cheng, F. Wu, C. Lv, et al., HtrA serine proteases in cancers: a target of interest for cancer therapy, Biomed. Pharmacother. 139 (2021) 111603, https://doi.org/10.1016/j.biopha.2021.111603 (Epub 20210508. PubMed PMID: 34243596).
[49] L. Feng, Z. Li, Y. Xiong, T. Yan, C. Fu, Q. Zeng, et al., HtrA2 independently predicts poor prognosis and correlates with immune cell infiltration in hepatocellular carcinoma, J. Oncol. 2023 (2023) 4067418, https://doi.org/10.1155/2023/4067418 (Epub 20230117. PubMed PMID: 36704205; PubMed Central PMCID: PMC9873461).
[50] F.G. Pruefer, F. Lizarraga, V. Maldonado, J. Melendez-Zajgla, Participation of Omi Htra2 serine-protease activity in the apoptosis induced by cisplatin on SW480 colon cancer cells, J. Chemother. 20 (3) (2008) 348–354, https://doi.org/10.1179/joc.2008.20.3.348 (PubMed PMID: 18606591).
[51] G. Brummer, D.S. Acevedo, Q. Hu, M. Portsche, W.B. Fang, M. Yao, et al., Chemokine signaling facilitates early-stage breast cancer survival and invasion through fibroblast-dependent mechanisms, Mol. Cancer Res. 16 (2) (2018) 296–308, https://doi.org/10.1158/1541-7786.Mcr-17-0308 (Epub 20171113. PubMed PMID: 29133591; PubMed Central PMCID: PMC5805627.).
[52] Z.H. Zhu, Y.P. Yu, Z.L. Zheng, Y. Song, G.S. Xiang, J. Nelson, et al., Integrin alpha 7 interacts with high temperature requirement A2 (HtrA2) to induce prostate cancer cell death, Am. J. Pathol. 177 (3) (2010) 1176–1186, https://doi.org/10.2353/ajpath.2010.091026 (Epub 20100722. PubMed PMID: 20651226; PubMed Central PMCID: PMC2928952).
[53] Z. Feng, Y. Ou, L. Hao, The roles of glycolysis in osteosarcoma, Front. Pharmacol. 13 (2022) 950886, https://doi.org/10.3389/fphar.2022.950886 (Epub 20220817. PubMed PMID: 36059961; PubMed Central PMCID: PMC9428632.).